JOURNAL OF VIROLOGY, Nov. 1994, p. 7507–7515
0022-538X/94/$04.00+0

Vol. 68, No. 11

Mouse Neurovirulence Determinants of Poliovirus Type 1 Strain LS-a Map to the Coding Regions of Capsid Protein VP1 and Proteinase $2A^{pro}$

HUI-HUA LU,[1]* CHEN-FU YANG,[2] ANDREW D. MURDIN,[3] MICHEL H. KLEIN,[3] JAMES J. HARBER,[1]† OLEN M. KEW,[2] AND ECKARD WIMMER[1]

Department of Molecular Genetics and Microbiology, School of Medicine, State University of New York at Stony Brook, Stony Brook, New York 11794-5222[1]; Division of Viral and Rickettsial Diseases, National Center for Infectious Diseases, Centers for Disease Control and Prevention, Atlanta, Georgia 30333[2]; and Connaught Laboratories Ltd., Willowdale, Ontario, Canada M2R 3T4[3]

Received 13 June 1994/Accepted 15 August 1994

Poliovirus type 1 strain LS-a [PV1(LS-a)] is a PV variant adapted to mice by multiple passages through mouse and monkey tissues. To investigate the molecular basis underlying mouse neurovirulence of PV1(LS-a), a cDNA of the viral genome containing nucleotides 112 to 7441 was cloned, and the nucleotide sequence was determined. Compared with that of the mouse avirulent progenitor PV1(Mahoney), 54 nucleotide changes were found in the genome of the PV1(LS-a) virus, resulting in 20 amino acid substitutions in the virus polyprotein. Whereas the nucleotide changes were scattered throughout the genome, the amino acid substitutions were largely clustered in the capsid proteins and, to a certain extent, in the virus proteinase $2A^{pro}$. By in vitro mutagenesis, PV1(LS-a)-specific capsid mutations were introduced into a cDNA clone of PV1(Mahoney). We show that neither the individual amino acid mutations nor combinations of mutations in the region encoding VP1 conferred to PV1(Mahoney) the mouse-adapted phenotype of PV1(LS-a). Chimeric cDNA studies demonstrated that a recombinant type 1 virus containing the PV1(LS-a) sequence from nucleotide 2470 to nucleotide 3625 displayed a neurovirulent phenotype in mice. Further dissection of this region revealed that mouse neurovirulence of PV1(LS-a) was determined by multiple mutations in regions encoding both viral proteinase $2A^{pro}$ and capsid protein VP1. The mouse neurovirulent viruses, PV1(LS-a), W1-M/LS-Pf [nucleotides 496 to 3625 from PV1(LS-a)], and W1-M/LS-NP [nucleotides 2470 to 3625 from PV1(LS-a)], showed increased sensitivity to heat treatment at 45°C for 1 h. Surprisingly, the thermolabile phenotype was also displayed by a recombinant of PV1(Mahoney) carrying a PV1(LS-a) DNA fragment encoding the N-terminal portion of $2A^{pro}$. This suggests that base substitutions in the region encoding $2A^{pro}$ affected capsid stability, thereby contributing to the neurovirulence of the virus in mice.

Enigmatic in studies of the pathogenesis of poliovirus (PV) is the mechanism by which mouse-adapted strains cause neurologic symptoms in mice. These strains cannot infect any cultured rodent cells, such as mouse L cells, unless the cells have been transformed with cDNAs (16, 24) or with the gene (3) specifying the human PV receptor (*h*PVR). Apparently, the mouse homolog of *h*PVR cannot replace that receptor for the mouse-adapted PV (27). Therefore, at least at the level of cell culture, the barrier to infection resides in the absence of a suitable cell surface protein facilitating uptake of the mouse-adapted virus. When injected intraspinally or intracerebrally, however, these strains may kill the mouse, although they do not cause the typical syndrome of poliomyelitis (8a).

PV is the prototype virus of the genus *Enterovirus* of the family *Picornaviridae*. It is a small, nonenveloped plus-strand RNA virus. The icosahedral particle consists of 60 copies each of the capsid proteins VP1, VP2, VP3, and VP4. The three largest molecules (VP1 to VP3) form the outer surface, while VP4 is a capsid-internal protein (13). The genome of PV is a single copy of single-stranded RNA of plus-strand polarity encoding a single polypeptide, the polyprotein (Fig. 1A) (15, 34). The polyprotein is processed by virus-encoded proteinases into numerous polypeptides, including the capsid-specific proteins VP0 (the precursor to VP4 and VP2), VP3, and VP1 (15, 32). Except for the "maturation cleavage" of VP0 (10), proteolytic processing is catalyzed by the proteinases $2A^{pro}$, $3C^{pro}$, and $3CD^{pro}$ (8, 11). The coding region for $2A^{pro}$ maps directly adjacent to the capsid protein region P1 (Fig. 1A), and, indeed, $2A^{pro}$ cleaves the polyprotein cotranslationally into the structural (P1) and nonstructural (P2 and P3) polypeptides (12, 31, 41).

PV exists in three serotypes (PV1, PV2, and PV3). All three are able to cause poliomyelitis in humans or, after experimental infection, in monkeys. The narrow host range is determined by the specificity of the interaction between *h*PVR (4, 16, 24) or its monkey homolog (17) with the poliovirion. These receptors, whose normal function is unknown, are immunoglobulin-like polypeptides consisting of three extracellular domains (V-C2-C2). They perform a dual function in PV infection: attachment of the virus to the cell surface and destabilization of the virion, leading to the formation of A particles (7). The genetics of expression of the PVR gene, resulting in the synthesis of several splice variants, is complex, and the distribution of the receptor protein(s) in human tissue, as a determinant of viral tissue tropism, is poorly understood (43).

Most wild-type PV strains do not proliferate in mice,

* Corresponding author. Phone: (516) 632-8787. Fax: (516) 632-8891.

† Present address: Department of Biology, California Institute of Technology, Pasadena, CA 91125.

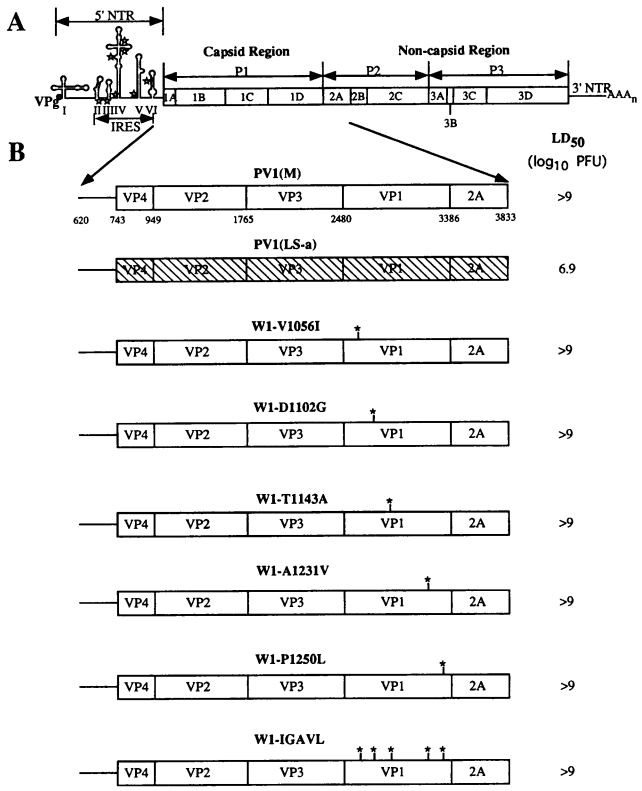

FIG. 1. Genotype and mouse neurovirulence of the wild-type and mutant PVs. (A) Gene organization of PV. Domains of the 5′-nontranslated region (5′ NTR) are indicated by Roman numerals. Stars indicate the positions of noninitiating AUG triplets. P1 is the precursor of the capsid proteins; P2 and P3 are the precursors of the noncapsid proteins. 1A, 1B, 1C, and 1D are capsid proteins VP4, VP2, VP3, and VP1, respectively. (B) Genotype and mouse neurovirulence (*mn*) phenotype of the wild-type and mutant viruses. The genome segments from nt 620 to 3833 of the viruses are enlarged, and the nucleotide positions are indicated by numbers under the bar. The PV1(M) sequence is indicated by an open bar, and the PV1(LS-a) sequence is indicated by a hatched bar. Amino acid changes are indicated by stars. The mouse neurovirulence of each virus was assayed with young Swiss Webster mice as described in Materials and Methods. LD$_{50}$, 50% lethal dose.

presumably for lack of receptors (14). An exception may be MEF 1, a type 2 PV (PV2) strain reported to be mouse neurovirulent without extended prior passage in mouse brain (39). Other PV2 strains were adapted to proliferate in the mouse central nervous system (CNS), the best known being PV2(Lansing) [PV2(L)] (2). In 1953, Li and Schaeffer reported the isolation of a mouse-adapted, neurovirulent strain of PV type 1 [PV1(LS-a)] (20).

Attempts to decipher the determinants of mouse neurovirulence of PV have yielded a very complex pattern. These experiments have followed a strategy to convert PV1(Mahoney) [PV1(M)], a wild-type strain that does not cause apparent disease in mice, to the mouse neurovirulent phenotype (*mn*), either by genetic exchange of gene segments between PV1(M) and PV2(L) (23, 29) or by passage in the CNS of mice (6, 28). *mn* PV1(M) variants were obtained by the exchange of a limited number of amino acids in a loop well exposed at the surface of the virion (BC loop of VP1) (23, 29) or, remarkably, as the result of single-amino-acid exchanges in VP1 or VP2 internal to the capsid (6, 28). We have begun to analyze *mn* determinants of PV1(LS-a) and the disease syndrome that this strain causes in normal mice. Here, we report the unexpected finding that *mn* is determined by mutations mapping to the coding regions of VP1 plus δ2A^{pro} (δ2A^{pro} contains the first 80 amino acids of 2A^{pro}).

MATERIALS AND METHODS

Bacterial strains and plasmids. *Escherichia coli* DH5α and C600 were used as hosts for plasmid transformation and propagation. Plasmid pT7PVM is a derivative of pT7XL, a full-length PV1(M) clone (5). Plasmid pBH6-5 is a pBR322-based vector containing PV1(M) sequence from nucleotide (nt) 1172 (the *Nru*I site) to nt 2954 (the *Sna*BI site). To clone the cDNA of PV1(LS-a), pBH6-5 was cut with *Nru*I and *Sna*BI and the PV1(M) DNA fragment from nt 1172 to nt 2954 was replaced with in vitro-synthesized PV1(LS-a) cDNA.

Virus and cells. The mouse-adapted PV1(LS-a) was originally generated from PV1(M) by Li and Schaeffer (21). The virus stock kept at the Centers for Disease Control and Prevention, Atlanta, Ga., was used as seed in this study.

HeLa R19 cell monolayers or HeLa S3 suspension cultures were maintained in Dulbecco's modified Eagle medium supplemented with 5% fetal bovine serum. For virus amplification, HeLa cells were infected with viruses at a multiplicity of infection of between 5 and 10 PFU per cell. The infected cells were incubated in Dulbecco's modified Eagle medium–5% fetal bovine serum and harvested upon the appearance of the cytopathic effect. After three cycles of freezing and thawing, the released virus was clarified by low-speed centrifugation and concentrated by spinning at 30,000 rpm in a Beckman 50.2 Ti rotor at 22°C for 3 h. When necessary, the virus was further purified through CsCl gradient centrifugation at 40,000 rpm (Beckman SW 50.1 rotor) at 22°C for 18 h. The titers of the virus stocks were determined by standard plaque assay on HeLa R19 monolayers.

Construction of the cDNA clone of PV1(LS-a). PV1(LS-a) virus RNA was isolated from CsCl-purified PV1(LS-a) virus stock by standard methods. A cDNA synthesis kit (Boehringer Mannheim) was used to synthesize the cDNA of the PV1 (LS-a) virus as instructed by the manufacturer. Briefly, the virus RNA (5 μg) was annealed to a deoxyribosylthymine oligonucleotide primer and reverse transcribed to produce the first strand of cDNA. The second-strand synthesis was carried out by RNase H and *E. coli* DNA polymerase I. The resulting double-stranded DNA was blunt ended by T4 DNA polymerase and ligated to the pBH6-5 vector blunted by *Sna*BI and *Nru*I restriction, yielding pBH75LS-a.

DNA manipulations. DNA cloning was accomplished by standard procedures (38). The recombinants between PV1(M) and PV1(LS-a) were constructed by exchanging the corresponding DNA fragments digested with common restriction enzymes. Point mutations were generated in subclones either by PCR of the corresponding sequence from the PV1(LS-a) cDNA or by site-directed mutagenesis that used uridine-enriched single-strand DNA (19). After sequence analysis, the mutated DNA fragments were cloned back into the full-length cDNA clone.

Plaque assay. The infectivity of all of the virus stocks was titrated by plaque assay on HeLa R19 cell monolayers seeded on six-well plates. Serial dilutions (10-fold) of virus stocks were made with phosphate-buffered saline. Three hundred microliters of each dilution was applied to the monolayer and then adsorbed at room temperature for 30 min. The cells were then overlaid with 1.4% Noble agar containing 5% fetal bovine

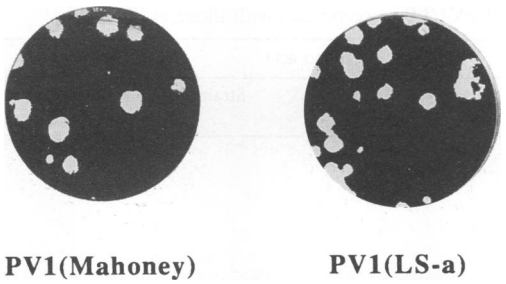

FIG. 2. Plaque phenotypes of PV1(M) and PV1(LS-a) on HeLa cell monolayers. The plates were incubated at 37°C for 48 h, followed by 1% crystal violet staining.

serum and 1× modified Eagle medium. After 48 h of incubation at 37°C, the plaques were developed by staining with 1% crystal violet.

RNA and DNA sequencing. Five to 10 μg of total cytoplasmic RNA isolated from virus-infected cells was used for each RNA sequencing reaction. RNA sequencing was accomplished by using an RNA sequencing kit (Boehringer Mannheim) and following the instructions provided by the manufacturer.

The P1 region of the PV1(LS-a) genomic cDNA was sequenced with an Applied Biosystems model 373A DNA sequencing system. The DNA was purified by two cycles of CsCl gradient banding and sequenced according to the manufacturer's protocol for *Taq* DyeDeoxy terminator cycle sequencing. The rest of the genome was sequenced by using the PRISM dye terminator cycle sequencing kit with the same auto sequencing system. The sequencing was performed in both directions, and each nucleotide position was sequenced at least twice from both strands.

Transcription and transfection assays. For the production of infectious RNA transcripts in vitro, 2 μg of full-length cDNA was linearized by a unique restriction enzyme downstream of the virus genome. RNA transcripts were produced from the linear DNA by T7 RNA polymerase in an in vitro system described previously (42).

HeLa R19 monolayers cultured in 35-mm-diameter plates were transfected with approximately 200 ng of RNA transcripts in the presence of 0.5 mg of DEAE-dextran per ml in HeBSS buffer (42 mM HEPES, 270 mM NaCl, 9.6 mM KCl, 1.4 mM Na_2HPO_4, and 11 mM glucose) and incubated at room temperature for 30 min (42). The RNA mixture was then removed, and the cells were grown in 2 ml of Dulbecco's modified Eagle medium containing 2% fetal bovine serum at 37°C until the cytopathic effect appeared.

Mouse neurovirulence assay. The mouse neurovirulence of each virus was tested on 22- to 24-day-old female Swiss Webster mice. Groups of six mice were intracerebrally injected with 30 μl of purified virus suspended in phosphate-buffered saline. The injected mice were observed daily for 3 weeks for paralysis and death. The 50% lethal dose of the viruses was determined by injecting serially (10-fold) diluted virus and was calculated as described by Reed and Muench (35).

RESULTS

Nucleotide sequence of the genome of PV1(LS-a). PV1(M), albeit highly virulent in primates, is avirulent in rodents. However, repeated passage of the virus in monkey tissues as well as in mouse CNS resulted in the emergence of PV1(LS-a), one of the few PV1 strains that caused disease in mice (20). The plaque phenotype of the PV1(LS-a) virus assayed on HeLa cells was slightly smaller than that of PV1(M) (Fig. 2), but the virus grew in cultured cells to a level comparable to that of PV1(M) (data not shown). There were no apparent differences observed in cleavage patterns of PV1(LS-a) polyprotein, and that was true particularly for the processing of the capsid P1 precursor and the composition of the virion proteins (data not shown). The 50% lethal dose of a plaque-purified isolate of PV1(LS-a) was found to be $10^{6.9}$ PFU (Fig. 1B). To analyze the molecular basis underlying the mouse-adapted phenotype of this virus, a cDNA clone was generated from the genomic RNA of PV1(LS-a). The cDNA was sequenced from nt 113 to the 3′ end of the genome. A total of 54 nt substitutions (13 transversions and 41 transitions) accumulated in the virus genome during mouse adaptation. Twenty of these yielded amino acid changes (Table 1). Whereas the base changes were scattered throughout the genome, the amino acid substitutions were largely clustered in the region encoding the capsid proteins and the virus proteinase $2A^{pro}$. Moreover, approximately 50% of the amino acid changes were specific for PV1(LS-a); the rest could also be found in PV1(Sabin) and some other strains. It is noteworthy that five of six PV1(LS-a)-specific capsid amino acid changes occurred in VP1, the most exposed protein of the capsid proteins. In addition, four base changes were identified in the 5′ nontranslated region that was sequenced in this study. Among these, the mutations at nt 140 and 189 were located in the 5′-terminal region of the internal ribosomal entry site, a *cis*-acting genetic element of picornavirus that confers cap- and 5′ end-independent translation of the virus mRNA (44). It is not clear if these point mutations in the internal ribosomal entry site would affect virus RNA translation inside the mouse CNS; however, they appeared to have no effect on virus growth in cultured HeLa cells (data not shown). Furthermore, a guanosine-to-adenosine change at nt 4124 resulted in a cleavage site mutation (Gln-Gly→Gln-Ser) at the border between the virus polypeptides 2B and 2C, in contrast to a Gln-Gly pair found at this cleavage site of all the other PV strains.

PV1(LS-a)-specific mutations that accumulated in VP1 were not sufficient to confer the mouse neurovirulent (*mn*) phenotype. The nucleotide sequence of the PV1(LS-a) cDNA revealed a cluster of PV1(LS-a)-specific mutations yielding amino acid changes in capsid protein VP1 (Table 1). Most of these mutations were located either in the exposed surface loops on the apexes of the virion or close to the canyon, a depressed structure surrounding the fivefold axis of symmetry (Table 2). This canyon is the likely receptacle for *h*PVR (37). To determine whether any of these mutations could produce the *mn* phenotype, mutant PV1(M) clones bearing corresponding amino acid changes were constructed by site-directed mutagenesis. The resulting viruses were tested with Swiss Webster mice via an intracerebral route. Surprisingly, none of the point mutants caused any apparent disease in mice (Fig. 1B). To examine the possibility that these mutations additively contribute to the *mn* phenotype, a construct combining all five of the PV1(LS-a)-specific capsid mutations was engineered. However, the combination of the mutations did not increase mouse neurovirulence either (Fig. 1B). As will be shown below, recombinant viruses containing PV1(LS-a)-specific sequences of VP1 or the entire P1 failed to cause paralysis in mice, an observation suggesting that PV1(LS-a) capsid mutations by themselves were not sufficient to confer mouse neurovirulence for PV1 (see viruses W1-M/LS-NB in Fig. 3B and W1-M/LS-PB in Fig. 3A). However, the capsid mutations did play a role in mouse infectivity, since chimeric PV containing PV1(LS-a) 2A mutations but lacking the PV1(LS-a)-specific capsid mutations also failed to cause paralysis in mice (e.g.,

TABLE 1. Nucleotide and amino acid substitutions in the genome of PV1(LS-a) compared with those in PV1(M)

Nucleotide			Amino acid			
Position	PV1(M)	PV1(LS-a)	Position	PV1(M)	PV1(LS-a)	Strain(s) with the same amino acid change as PV1(LS-a)
Δ5′ nontranslated region (nt 113–742)						
140	T	G				
189	C	T				
649	C	T				
674	G	T				
VP4, 935	G	T	65	Ala	Ser	All other strains
VP2						
1072	T	C				
1329	T	C	130	Val	Ala[a]	
1490	C	T	181	Leu	Phe	PV1(S)[b], PV2(L), PV2(S)
VP3						
1547	C	T				
1885	A	T				
1933	C	T				
1944	C	A	60	Thr	Lys	PV1(S)
2353	T	C				
2438	T	A	224	Leu	Met	PV1(S)
VP1						
2545	A	G				
2585	A	G	36	Thr	Ala	All other strains
2645	G	A	56	Val	Ile[a]	
2784	A	G	102	Asp	Gly[a]	
2879	C	T	134	Leu	Phe	All other strains
2906	A	G	143	Thr	Ala[a]	
3135	A	G	219	Asp	Gly	PV2(L), PV2(S)
3163	T	C				
3171	C	T	231	Ala	Val[a]	
3228	C	T	250	Pro	Leu[a]	
2A						
3445	C	T				
3460	T	A	25	Asp	Glu	All other strains
3492	G	A	36	Ser	Asn	PV1(S), PV2(S), PV3(Le),[c] PV3(S)
3514	A	G				
3594	A	G	70	Tyr	Cys[a]	
2B						
3896, 3898	A, C	G, A	22	Ser	Gly	All other strains
3931	C	T				
4003	C	T				
4117	C	T				
2C						
4124	G	A	1	Gly	Ser[a]	
4143	A	G	7	Lys	Arg[a]	
4174	C	A				
4186	G	A				
4339	C	T				
4444	T	C				
5107	T	C				
3A						
5248	C	T				
5317	C	T				
3B, 5420	C	A				
3C						
5440	A	G				
5506	A	G				
5839	T	C				

Continued on following page

TABLE 1—*Continued*

Nucleotide			Amino acid			
Position	PV1(M)	PV1(LS-a)	Position	PV1(M)	PV1(LS-a)	Strain(s)
3D						
6373	C	T				
6679	T	C				
6820	A	T	278	Lys	Asn[a]	
7069	T	C				
7198	T	A				
7303	T	A				
3′ nontranslated region,						
7410	T	C				

[a] PV1(LS-a)-specific amino acid substitutions; an additional G-2245→A transition generating a synonymous codon was identified in an independent sequencing of the P1 region of PV1(LS-a) genomic RNA (14a).
[b] S, Sabin.
[c] Le, Leon.

virus W1-M/LS-BP in Fig. 3B). In conclusion, these results suggested that the amino acid substitutions that accumulated in the region encoding the PV1(LS-a) capsid were necessary but not sufficient to confer the *mn* phenotype.

A major host range determinant resides in the region encoding VP1 and the N-terminal portion of 2A^{pro}. To further map the determinant of PV1(LS-a) mouse neurovirulence, a series of chimeric type 1 clones were constructed by replacing various DNA segments of PV1(M) with the corresponding segments of PV1(LS-a). The resulting chimeras were propagated on HeLa cells and found to have plaque phenotypes more or less similar to that of PV1(LS-a). Subsequently, they were assayed for their abilities to cause paralysis and death in mice. Two of the chimeric viruses, W1-M/LS-Pf and W1-M/LS-NP, exhibited the *mn* phenotype (Fig. 3B), whereas other chimeras that contained fragments encoding various regions of P1 of PV1(LS-a) did not cause any apparent disease (Fig. 3). W1-M/LS-Pf and W1-M/LS-NP harbored nt 496 to 3625 and 2470 to 3625 of PV1 (LS-a), respectively. W1-M/LS-NP was of particular interest because it identified the smallest segment of the PV1(LS-a) genome that conferred mouse neurovirulence. Further division of the PV1(LS-a) segment nt 2470 to 3625 into nt 2470 to 3236 and nt 3236 to 3625 resulted in two chimeras (W1-M/LS-NB and W1-M/LS-BP) that did not exhibit any pathogenic effect in mice. W1-M/LS-NB and W1-M/LS-BP contained the PV1(LS-a) sequences encoding VP1 and the N-terminal portion of 2A^{pro}, respectively, suggesting that the mouse neurovirulence of PV1(LS-a) was determined by multiple, nonseparable mutations in this region. This was further confirmed by another set of chimeras, W1-M/LS-NSn [which contained PV1(LS-a) nt 2470 to 2954] and W1-M/LS-SnP [PV1(LS-a) nt 2954 to 3625], both of which were mouse avirulent (Fig. 3B). We therefore conclude that the mouse neurovirulence of PV1(LS-a) was determined by mutations from two loci: the region encoding the viral capsid protein VP1 and the region encoding viral proteinase 2A^{pro}.

Thermostability of the wild-type and chimeric viruses. PV1(M) is relatively resistant to inactivation at 45°C. We were interested in determining whether the mutations that accumulated during multiple passages in monkey tissue and mouse CNS influenced the thermostability of PV1(LS-a). In this study, wild-type PV1(M), PV1(LS-a), and a series of Mahoney/LS-a chimeric viruses were incubated at 45°C for 1 h, and the residual infectivities were examined by plaque assay. Untreated control samples were assayed at the same time. As shown in Fig. 4, the titer of PV1(M) was reduced by approximately 1 log during heat treatment, whereas that of PV1(LS-a) lost approximately 5 logs of infectivity, a result indicating that PV1(LS-a) was highly thermolabile. In general, the virus variants expressing the *mn* phenotype were also thermolabile (LS-a, M/LS-PF, and M/LS-NP), and these variants all contained the δ2A^{pro} segment harboring the five PV1(LS-a)-specific mutations. Analysis of the nonneurovirulent variants revealed the surprising result that the increased thermolability correlated with the presence or absence of the PV1(LS-a)-specific δ2A^{pro} segment (M/LS-BP versus -NB, -NN, or -NS). Specifically, W1-M/LS-BP, a virus whose genotype is like that of PV1(M) except for the PV1(LS-a)-specific gene segment encoding 2A^{pro}, lost 5 logs of infectivity within 1 h at 45°C. It appears that the numerous mutations in the PV1(LS-a) capsid proteins had little effect on the sensitivity of the virion to heat. This suggests that the increased thermolability of PV1(LS-a) may result from specific RNA-protein interactions destabilizing the virus capsid.

DISCUSSION

Wild-type strains of PV are neurovirulent in transgenic mice expressing *h*PVR (18, 36). For virologists, the explanation for the extended host range is straightforward because the *mn* phenotype is not related to an altered genotype of the virus but is related to that of the host. In contrast, adaptation of PV strains to express an *mn* phenotype in normal mice is due to genetic changes of the virus. It now appears that with every genetic analysis of independently isolated mouse-adapted PV strains, the phenomenon of mouse neurovirulence is rendered more complicated. Even more complex are the disease syndromes produced by these PV variants, because none of them causes typical poliomyelitis in normal mice (8a).

Original analyses of the mouse-adapted strain PV2(L) mapped *mn* determinants to the BC loop of VP1 (23, 29), a well-exposed structure located near the fivefold axis above the canyon of the virion (Fig. 5). The VP1 BC loop is a neutralization antigenic site (N-AgIa) (25), while the canyon is considered to be the receptacle for the receptor (37) (for further references, see reference 1). Indeed, monoclonal antibodies binding to N-AgIa prevent attachment of the virus to host cells (1). Antigenic hybrid viruses consisting of PV1(M) carrying six PV2(L)-specific amino acids in the VP1 BC loop grow to wild-type levels in HeLa cells (23, 29), and their crystal structure differs from that of PV1(M) mainly in the VP1 BC

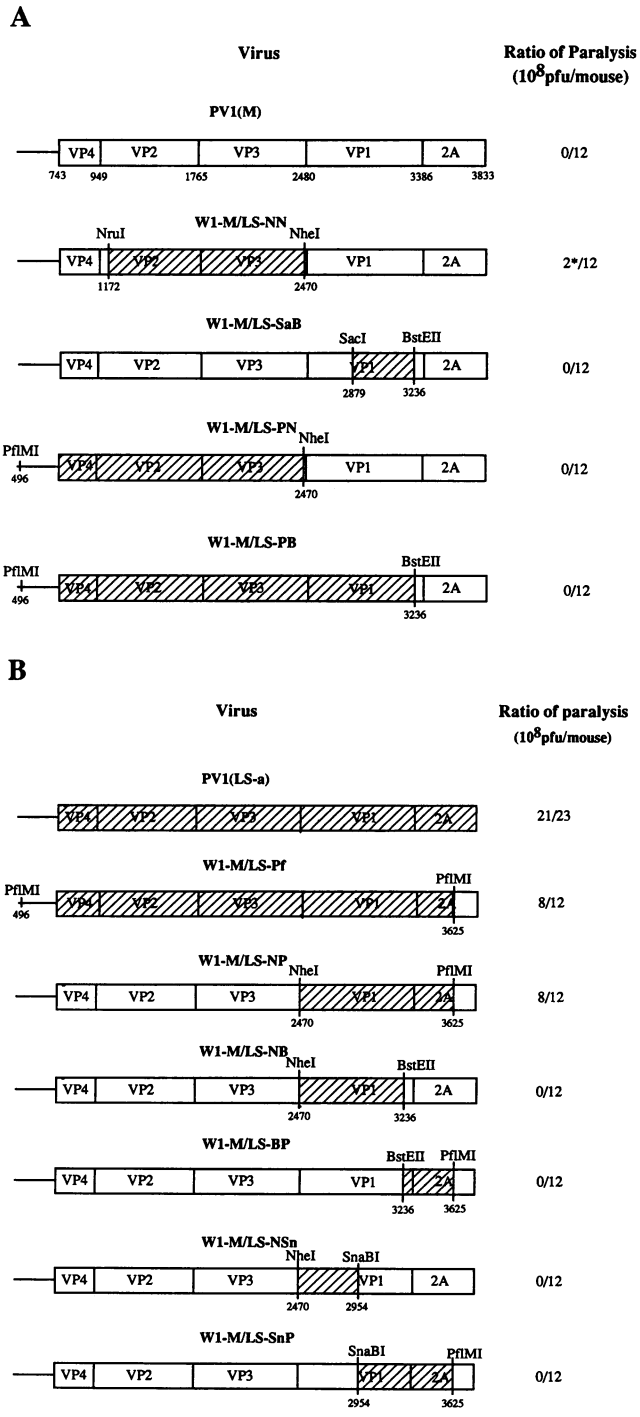

FIG. 3. Enlarged genome segments (nt 490 to 3833) demonstrating the genotypes of PV1(M) (open bars), PV1(LS-a) (hatched bars), and the chimeras. The restriction sites used to construct the chimeric viruses are indicated above the bars. The *Sac*I site at nt 2879 was introduced by in vitro mutagenesis. (A) Chimeric virus with PV1(LS-a) sequences encoding different regions of the capsid proteins. (B) Chimeric viruses demonstrated a multigenic, nondividable host range determinant that was contributed from the regions encoding VP1 and $2A^{pro}$. The asterisk indicates that the front limbs of the mice were slightly paralyzed.

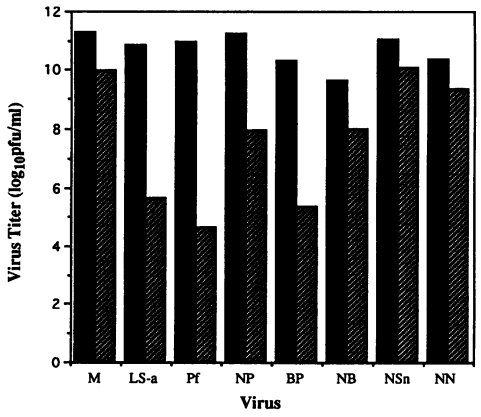

FIG. 4. Thermostability of the wild-type and chimeric PVs. The viruses were incubated at 45°C for 1 h prior to plaque assays. The titers of the heat-treated viruses are indicated by hatched bars (45°C), and those of the untreated viruses are indicated by solid bars (4°C). M, PV1(M); LS-a, PV1(LS-a); Pf, NP, BP, NB, NSn, and NN, chimeric viruses (structures illustrated in Fig. 3).

loop region (45). It was therefore suggested that the *mn* phenotype of PV2(L) was probably related to the ability of the BC loop of VP1 to interact with an unknown mouse receptor.

Subsequent studies of *mn* strains of PV1(M) that were obtained by passages in mouse CNS revealed, surprisingly, that very few mutations in the capsid other than the VP1 BC loop, and even a single mutation in VP1 or VP2, could produce an *mn* phenotype, although the mutations were not located at the surface of the virus shell (6, 28). These observations have led to the hypothesis that mutations affecting capsid protein interactions, such as protomer-protomer association or VP4 interaction with other capsid proteins, contribute to the PV *mn* phenotype in normal mice.

The numerous mutations in the capsid proteins of the mouse-adapted strain PV1(LS-a), however, are not sufficient to produce the *mn* phenotype (Fig. 1B and Fig. 3). This virus, whose parental strain is PV1(M), was isolated after 14 passages in monkey testicular and kidney tissue cells and 60 passages through the mouse CNS. It accumulated 54 point mutations with the expected higher frequency of transitions over transversions (44). The frequencies of base changes of regions encoding capsid and noncapsid proteins were found to be similar, although there were many fewer amino acid substitutions in noncapsid proteins than in capsid proteins. Exceptionally, the coding region for the virus proteinase $2A^{pro}$ accumulated five base changes; three of these resulted in amino acid changes. Another peculiar mutation in PV1(LS-a) was that of the proteolytic cleavage site between polypeptides 2B and 2C from Gln-Gly to Gln-Ser. In all wild-type PVs analyzed, proteolytic processing of the polyprotein catalyzed by proteinase $3C^{pro}$ or $3CD^{pro}$ occurs at Gln-Gly amino acid pairs (8, 11). The only other exception reported so far is a cleavage site between polypeptides 2C and 3A in PV2(W-2), which is also a Gln-Ser pair (33). Both PV1(LS-a) and PV2(W-2) are mouse-adapted viruses generated by passage through mouse CNS. However, whether the identical change of the P1′ position in cleavage sites of these viruses is significant or coincidental remains an open question.

Thirteen of 20 amino acid changes in the PV1(LS-a) polyprotein were located in the capsid proteins. The majority of the mutations occurred in VP1, including five of the six PV1(LS-a)-specific capsid mutations. The general location of

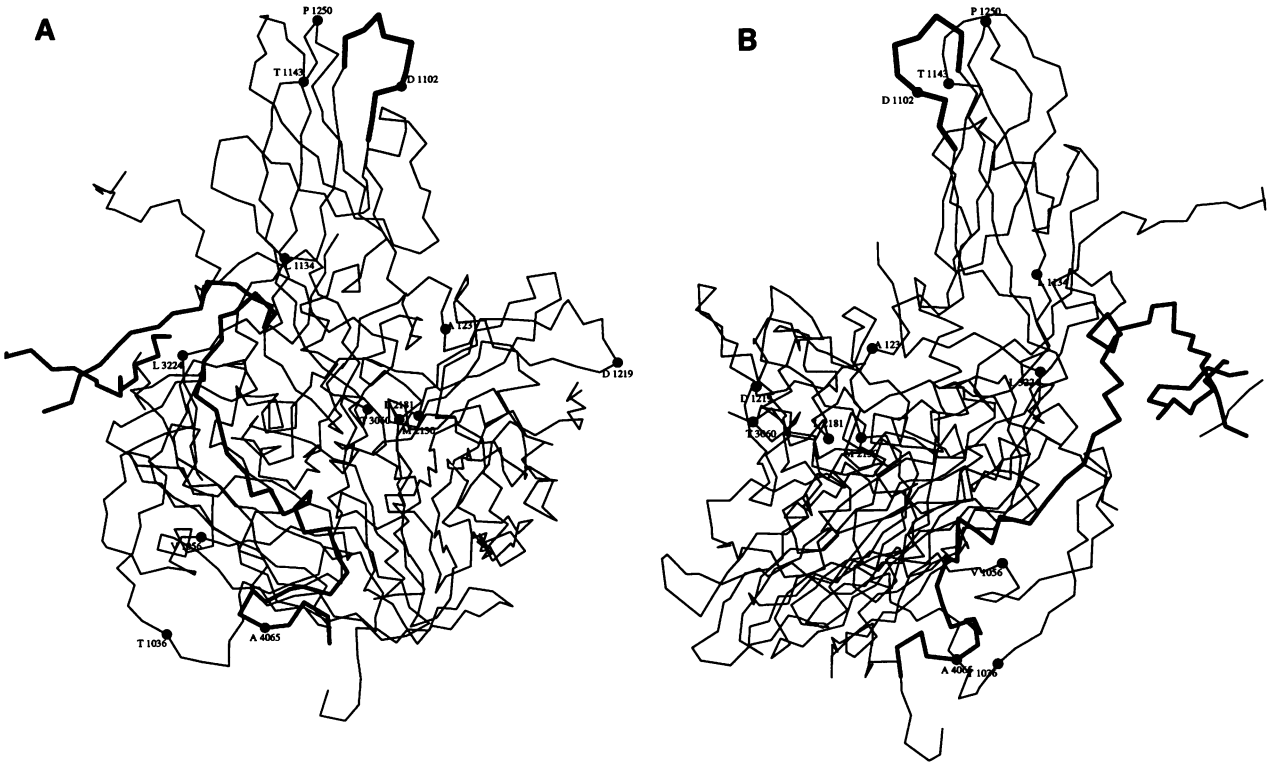

FIG. 5. Mapping of the capsid mutations accumulated in PV1(LS-a) on an α-carbon model of a protomer, viewed from the front (A) and side (B) of the virion. The display was generated by the program Insight II with a Silicon Graphics computer (model IRIS4D). The coordinates for PV (13) were obtained from Brookhaven Protein Data Bank. Sixty protomers, each consisting of a single copy of VP1 to VP4, constitute a poliovirion. VP4 and the BC loop of VP1 (on the top of the structure model) are highlighted. Amino acid substitutions are indicated by black dots. A four-digit nomenclature is used, in which the first digit specifies the capsid protein and the remaining digits denote the position of the amino acid within the protein (e.g., 1250 indicates residue 250 of VP1).

the capsid mutations in a protomer is shown in Fig. 5. Approximately 30% of these, almost all of which are PV1 (LS-a) specific, are located on the virion surface; the rest are more or less internally positioned, including one mutation mapping to the internal capsid protein VP4. Some structural implications of the PV1(LS-a)-specific VP1 mutations are summarized in Table 2. Mutation V-1056→I is located near the threefold axis of symmetry, adjacent to residue E-1054. A single mutation (E-1054→G) has recently been reported to produce an *mn* phenotype in PV1(M) (28), an observation that contrasts with the V-1056→I mutation identified here that had no effect. D-1102→G, T-1143→A, and P-1250→L mapped to the surface of the apexes (Fig. 5) within or in the vicinity of the BC loop (N-AgIa), a site that can determine mouse neurovirulence (see above). The A-1231→V mutation is located on the rim of the canyon and may influence binding to the unknown mouse receptor. Although the mutations found in PV1(LS-a) VP1 by themselves are not sufficient to produce the *mn* phenotype, they are necessary because they act in conjunction with downstream sequences (in $2A^{pro}$).

TABLE 2. Structural properties of the PV1(LS-a)-specific VP1 mutations

Amino acid substitution	Location	% Solvent-accessible area	Interacting residues[a]
V-1056→I	Interior	2	1054–1055, 1057–1059, 4063
D-1102→G	VP1 BC loop	42	1100–1101, 1103–1104, 1169
T-1143→A	VP1 DE loop	33	1141–1142, 1144–1145, 1252–1254
A-1231→V	Rim of canyon	12	1209, 1211–1213, 1228–1233, 2141
P-1250→L	Apexes	26	1096, 1248–1252, 1142–1145[b]

[a] Residues within 5 Å (1 Å = 0.1 nm) in the same protomer.
[b] Residues within 5 Å of the neighboring protomer.

The most interesting result of the study presented here is the apparent involvement of the coding sequence of $2A^{pro}$ in mouse neurovirulence of PV1(LS-a). As mentioned, the PV1 (LS-a) $2A^{pro}$ sequence harbors three amino acid changes, a large fraction of the mutations mapping to the nonstructural regions (Table 1). Of the three amino acid changes, the Y-70→C mutation is unusual because Tyr-70 of $2A^{pro}$ is conserved among all sequenced strains of PV. PV proteinase $2A^{pro}$ has been implicated in several different processes of replication: cleavage of the structural from the nonstructural proteins of the polyprotein (8, 11, 41); inhibition of host cell protein synthesis (40); transactivation of translation (9), possibly by binding to the internal ribosomal entry site elements (22); and RNA replication (26). It is conceivable that the mutations in PV1(LS-a) $2A^{pro}$ created a protein with altered properties affecting any of the $2A^{pro}$ functions mentioned above (or hitherto uncovered functions) and that such altered properties influenced the *mn* phenotype. On the other hand, the PV1(LS-a) mutations in $2A^{pro}$ per se were not sufficient to confer the *mn* phenotype to PV1(M), but they rendered this

virus extremely thermolabile (Fig. 4). We consider it possible, therefore, that specific interactions between the RNA sequence specifying $2A^{pro}$ and the capsid proteins exist and that a modification of these interactions by point mutations destabilizes the virus, thereby contributing to the mouse neurovirulence of PV1(LS-a). If so, it is even possible that sequences mapping to the coding region of $2A^{pro}$ function as an encapsidation signal.

An alternative, less likely explanation of the effect of the $2A^{pro}$ mutations could be that one or a few molecules of $2A^{pro}$ are encapsidated in the poliovirion that, hitherto undetected, influence capsid stability. Encapsidation of nonstructural proteins into picornavirus virions has been suggested recently (30). Dissection of the PV1(LS-a) mutations in $2A^{pro}$ will allow us to identify their effects on virus replication, capsid stability, and mouse neurovirulence.

ACKNOWLEDGMENTS

We are grateful to S.-J. Yang, D. England, and B. Nottay for excellent technical assistance in DNA sequencing; M. de Crombrugghe for computer display of the capsid proteins; G. Bernhardt for expertise in DNA alignment and stimulating discussion; and A. Cuconati for reading the manuscript.

J.J.H. is a member of the interinstitutional Genetics Training Program of SUNY Stony Brook, Cold Spring Harbor Laboratory, and Brookhaven National Laboratory. This project was supported by National Institutes of Health grants AI15122 and CA28146 to E.W. and support from the World Health Organization to H.-H.L. This publication was also supported by National Institutes of Health grant 2 T32CA09176.

REFERENCES

1. **Altmeyer, R., A. D. Murdin, J. J. Harber, and E. Wimmer.** 1991. Construction and characterization of a poliovirus/rhinovirus antigenic hybrid. Virology **184:**636–644.
2. **Armstrong, C.** 1939. Successful transfer of the Lansing strain of poliomyelitis virus from the cotton rat to the white mouse. Public Health Rep. **54:**2302–2305.
3. **Bernhardt, G., J. A. Bibb, J. Bradley, and E. Wimmer.** 1994. Molecular characterization of the cellular receptor for poliovirus. Virology **199:**105–113.
4. **Bernhardt, G., J. Harber, A. Zibert, M. de Crombrugghe, and E. Wimmer.** 1994. The poliovirus receptor: identification of domains and amino acid residues critical for virus binding. Virology **203:** 344–356.
5. **Cao, X., R. J. Kuhn, and E. Wimmer.** 1993. Replication of poliovirus RNA containing two VPg coding sequences leads to a specific deletion event. J. Virol. **67:**5572–5578.
6. **Couderc, T., J. Hogle, H. Le Blay, F. Horaud, and B. Blondel.** 1993. Molecular characterization of mouse-virulent poliovirus type 1 Mahoney mutants: involvement of residues of polypeptides VP1 and VP2 located on the inner surface of the capsid protein shell. J. Virol. **67:**3808–3817.
7. **Crowell, R. L., and B. J. Landau.** 1983. Receptors in the initiation of picornavirus infections, p. 1–42. *In* H. Fraenkel-Conrat and R. R. Wagner (ed.), Comprehensive virology, vol. 18. Plenum Press, New York.
8. **Dougherty, W. G., and B. L. Semler.** 1993. Expression of virus-encoded proteinases: functional and structural similarities with cellular enzymes. Microbiol. Rev. **57:**781–822.

8a. **Gromeier, M., H.-H. Lu, and E. Wimmer.** Mouse neuropathogenic poliovirus strains cause damage in the central nervous system different from poliomyelitis. Submitted for publication.

9. **Hambidge, S. J., and P. Sarnow.** 1992. Translational enhancement of the poliovirus 5′ noncoding region mediated by virus-encoded polypeptide 2A. Proc. Natl. Acad. Sci. USA **89:**10272–10276.
10. **Harber, J. J., J. Bradley, C. W. Anderson, and E. Wimmer.** 1991. Catalysis of the poliovirus VP0 maturation cleavage is not mediated by serine 10 of VP2. J. Virol. **65:**326–334.
11. **Harris, K. S., C. U. T. Hellen, and E. Wimmer.** 1990. Proteolytic processing in the replication of picornaviruses. Semin. Virol. **1:**323–333.
12. **Hellen, C. U. T., M. Fäcke, H.-G. Kräusslich, C.-K. Lee, and E. Wimmer.** 1992. Characterization of poliovirus 2A proteinase by mutational analysis: residues required for autocatalytic activity are essential for induction of cleavage of eukaryotic initiation factor 4F polypeptide p220. J. Virol. **65:**4226–4231.
13. **Hogle, J. M., M. Chow, and D. J. Filman.** 1985. The three dimensional structure of poliovirus at 2.9 Å resolution. Science **229:**1358–1365.
14. **Holland, J.** 1961. Receptor affinities as major determinants of enterovirus tissue tropisms in humans. Virology **15:**312–326.

14a. **Kew, O. M., et al.** Unpublished data.

15. **Kitamura, N., B. L. Semler, P. G. Rothberg, G. R. Larsen, C. J. Adler, A. J. Dorner, E. A. Emini, R. Hanecak, J. Lee, S. van der Werf, C. W. Anderson, and E. Wimmer.** 1981. Primary structure, gene organization and polypeptide expression of poliovirus RNA. Nature (London) **291:**547–553.
16. **Koike, S., H. Horie, I. Ise, A. Okitsu, M. Yoshida, N. Iizuka, K. Takeuchi, T. Takegami, and A. Nomoto.** 1990. The poliovirus receptor protein is produced both as membrane-bound and secreted forms. EMBO J. **9:**3217–3224.
17. **Koike, S., I. Ise, Y. Sato, H. Yonekawa, O. Gotoh, and A. Nomoto.** 1992. A second gene for the African green monkey poliovirus receptor that has no putative N-glycosylation site in the functional N-terminal immunoglobulin-like domain. J. Virol. **66:**7059–7066.
18. **Koike, S., C. Taya, T. Kurata, S. Abe, I. Ise, H. Yonekawa, and A. Nomoto.** 1991. Transgenic mice susceptible to poliovirus. Proc. Natl. Acad. Sci. USA **88:**951–955.
19. **Kunkel, T. A.** 1985. Rapid and efficient site-specific mutagenesis without phenotypic selection. Proc. Natl. Acad. Sci. USA **82:**488–492.
20. **Li, C. P., and M. Schaeffer.** 1953. Adaptation of type 1 poliomyelitis virus to mice. Proc. Soc. Exp. Biol. Med. **82:**477–481.
21. **Li, C. P., and M. Schaeffer.** 1954. Isolation of a non-neurotropic variant of type 1 poliomyelitis virus. Proc. Soc. Exp. Biol. Med. **87:**148–153.
22. **Macadam, A. J., G. Ferguson, T. Fleming, D. M. Stone, J. W. Almond, and P. M. Minor.** 1994. Role for poliovirus protease 2A in cap independent translation. EMBO J. **13:**924–927.
23. **Martin, A., C. Wychowski, T. Couderc, R. Crainic, J. Hogle, and M. Girard.** 1988. Engineering a type 2 antigenic site on a type 1 capsid results in a chimeric virus which is neurovirulent for mice. EMBO J. **7:**2839–2844.
24. **Mendelsohn, C. L., E. Wimmer, and V. R. Racaniello.** 1989. Cellular receptor for poliovirus: molecular cloning, nucleotide sequence, and expression of a new member of the immunoglobulin superfamily. Cell **56:**855–865.
25. **Minor, P. D.** 1990. Antigenic structure of picornaviruses. Curr. Top. Microbiol. Immunol. **161:**121–154.
26. **Molla, A., A. V. Paul, M. Schmid, S. K. Jang, and E. Wimmer.** 1993. Studies on dicistronic polioviruses implicate viral proteinase $2A^{pro}$ in RNA replication. Virology **196:**739–747.
27. **Morrison, M. E., and V. R. Racaniello.** 1992. Molecular cloning and expression of a murine homolog of the human poliovirus receptor gene. J. Virol. **66:**2807–2813.
28. **Moss, E., and V. R. Racaniello.** 1991. Host range determinants located on the interior of the poliovirus capsid. EMBO J. **10:**1067–1074.
29. **Murray, M. G., J. Bradley, X.-F. Yang, E. Wimmer, E. G. Moss, and V. R. Racaniello.** 1988. Poliovirus host range is determined by a short amino acid sequence in neutralization antigenic site I. Science **241:**213–215.
30. **Newman, J. F., P. G. Piatti, B. M. Gorman, T. G. Burrage, M. D. Ryan, M. Flint, and F. Brown.** 1994. Foot-and-mouth disease virus particles contain replicase 3D. Proc. Natl. Acad. Sci. USA **91:**733–737.
31. **Nicklin, M. J. H., H.-G. Kräusslich, H. Toyoda, J. J. Dunn, and E. Wimmer.** 1987. Poliovirus polypeptide precursors: expression in vitro and processing by exogenous 3C and 2A proteinases. Proc. Natl. Acad. Sci. USA **84:**4002–4006.
32. **Nicklin, M. J. H., H. Toyoda, M. G. Murray, and E. Wimmer.** 1986. Proteolytic processing in the replication of polio and related

viruses. Bio/Technology **4**:33–42.
33. **Pevear, D. C., C. K. Oh, L. L. Cunningham, M. Calenoff, and B. Jubelt.** 1990. Localization of genomic regions specific for the attenuated, mouse-adapted poliovirus type 2 strain W-2. J. Gen. Virol. **71**:43–52.
34. **Racaniello, V. R., and D. Baltimore.** 1981. Molecular cloning of poliovirus cDNA and determination of the complete nucleotide sequence of the viral genome. Proc. Natl. Acad. Sci. USA **78**:4887–4891.
35. **Reed, L. J., and M. Muench.** 1938. A simple method for estimating fifty percent endpoints. Am. J. Hyg. **27**:493–497.
36. **Ren, R., F. Costantini, E. J. Gorgacz, J. J. Lee, and V. R. Racaniello.** 1990. Transgenic mice expressing a human poliovirus receptor: a new model for poliomyelitis. Cell **63**:353–362.
37. **Rossmann, M. G.** 1989. The canyon hypothesis. Hiding the host cell receptor attachment site on a viral surface from immune surveillance. J. Biol. Chem. **264**:14587–14590.
38. **Sambrook, J., E. F. Fritsch, and T. Maniatis.** 1989. Molecular cloning: a laboratory manual, 2nd ed. Cold Spring Harbor Laboratory, Cold Spring Harbor, N.Y.
39. **Schlesinger, R. W., I. M. Morgan, and P. K. Olitsky.** 1943. Transmission to rodents of Lansing type poliomyelitis virus originating in the Middle East. Science **98**:452–454.
40. **Sonenberg, N.** 1990. Poliovirus translation. Curr. Top. Microbiol. Immunol. **161**:23–47.
41. **Toyoda, H., M. J. H. Nicklin, M. G. Murray, C. W. Anderson, J. J. Dunn, F. W. Sudier, and E. Wimmer.** 1986. A second virus-encoded proteinase involved in proteolytic processing of poliovirus polyprotein. Cell **45**:761–770.
42. **van der Werf, S., J. Bradley, E. Wimmer, F. W. Studier, and J. J. Dunn.** 1986. Synthesis of infectious poliovirus RNA by purified T7 RNA polymerase. Proc. Natl. Acad. Sci. USA **78**:2330–2334.
43. **Wimmer, E., J. J. Harber, J. A. Bibb, M. Gromeier, H. H. Lu, and G. Bernhardt.** 1994. The poliovirus receptors, p. 1–24. *In* E. Wimmer (ed.), Cellular receptors for animal viruses. Cold Spring Harbor Laboratory Press, Cold Spring Harbor, N.Y.
44. **Wimmer, E., C. U. T. Hellen, and X. M. Cao.** 1993. Genetics of poliovirus. Annu. Rev. Genet. **27**:353–436.
45. **Yeates, T. O., D. H. Jacobson, A. Martin, C. Wychowski, M. Girard, D. J. Filman, and J. M. Hogle.** 1991. Three-dimensional structure of a mouse-adapted type 2/type 1 poliovirus chimera. EMBO J. **10**:2331–2341.